Electron Spin Resonance and Magnetic Relaxation Studies of Gadolinium(III) Complexes with Human Transferrin†

Patricia B. O'Hara*
Department of Chemistry, Amherst College, Amherst, Massachusetts 01002
Seymour H. Koenig
IBM Thomas J. Watson Research Center, Yorktown Heights, New York 10598
Received August 5, 1985

ABSTRACT: A human serum transferrin complex was prepared in which Gd(III) was substituted for Fe(III) at the two metal-binding sites. Characteristic changes upon metal binding in both the UV absorption of ligated tyrosines and the solvent proton longitudinal magnetic relaxation rates demonstrated 2/1 metal stoichiometry and pH-dependent binding constants. Binding studies were complicated both by binding of Gd(III) to nonspecific sites on transferrin at pH ≤7 and by complexation of the Gd(III) by the requisite bicarbonate anion at pH ≥6.0. A unique Gd(III) electron spin resonance spectrum, with a prominent signal at $g = 4.96$, was observed for the specific Gd(III)–transferrin complex. The major features of this spectrum were fit successfully by a model Hamiltonian which utilized crystal field parameters similar to those determined for Fe(III) in transferrin [Aasa, R. (1970) *J. Chem. Phys. 52*, 3919–3924]. The magnetic field dependence of the solvent proton relaxation rate was measured as a function of both pH and metal ion concentration. An observed biphasic dependence of the relaxation rate on metal concentration is attributed to either sequential metal binding to the two iron-binding sites with different relaxation properties or random binding to two sites that are similar but show conformationally induced changes in relaxation properties as the second metal is bound. The increase in the solvent proton relaxation rate with pH is consistent with a model in which a proton of a second coordination sphere water molecule is hydrogen bonded to a metal ligand which becomes deprotonated at pH 8.5.

Human serum transferrin is a glycoprotein of 80 kilodaltons (kDa)[1] that functions biologically to bind trivalent iron and transport it through the blood either to the reticulocytes, where the iron is incorporated into hemoglobin, or to the liver, where the iron is stored in ferritin and hemosiderin. A bicarbonate (or carbonate) anion is required for tight binding of the iron to the protein. Although transferrin has no subunit structure, preliminary X-ray crystallographic studies reveal a single chain with two homologous domains each of which presumably contains a metal-binding site (DeLucas et al., 1980). Spectroscopic studies have suggested that each metal site contains two to three tyrosines, one to two histidines, a water molecule (or hydroxide), and the synergistic bicarbonate anion (Aisen & Listowsky, 1980; Chasteen, 1983). Analysis of the complete amino acid sequence suggests that Tyr-185, Tyr-188, and His-207 and Tyr-514, Tyr-517, and His-535 contribute to the binding in the N- and C-terminal domains, respectively (MacGillivray et al., 1983). Most trivalent metals (including the lanthanides) and some divalent metals bind specifically to the iron-binding sites of the apoprotein, and information regarding site/site differences has been obtained from studies of these metal-substituted transferrins. Though similar in their overall structure and function, the two sites (labeled A and B and located in the C- and N-terminal halves of the protein, respectively) have been shown to have significant differences in the kinetics and pH dependence of iron binding (Kojima & Bates, 1979; Harris, 1977), thermal stabilities (Donovan & Ross, 1975), and VO(IV) and Eu(III) crystal field symmetries (Cannon & Chasteen, 1975; O'Hara & Bersohn, 1982).

Because of their luminescent properties, lanthanides have been particularly useful in the study of the metal-binding properties of transferrin (Luk, 1971; O'Hara et al., 1981; O'Hara & Bersohn, 1982). Here, we have investigated the utility of lanthanide protein complexes as models for native transferrin by comparing optical and magnetic structural information derived from Gd(III) and Fe(III) transferrins. Gd–Tf was prepared and characterized by UV absorption, ESR, and nuclear magnetic relaxation dispersion (NMRD), and extensive structural information about the local metal environment was obtained by these three complementary techniques. UV difference spectroscopy was used to follow the specific binding of metal to the protein and to determine the number of tyrosinate ligands according to the method of Pecararo et al. (1981); ESR gave information about the symmetry of the ligand field, and NMRD was used to learn about the accessibility of solvent to the metal ions.

The utility of Gd(III) ESR as a structural probe has been demonstrated previously (Stephens & Grisham, 1979; Reed et al., 1979). Most, if not all, inorganic and biological complexes of Gd(III) ($S = {}^7/_2$) studied by ESR to date have shown a major transition in the $g = 2.0$ region. This value for g indicates a highly symmetric electronic environment for Gd(III), as one would expect from the ${}^8S_{7/2}$ ground state and the near-octahedral orbital symmetry associated with a half-filled f shell. The symmetry of the "buried" 4f level in these systems

† This work was supported in part by a grant from E. I. du Pont de Nemours and Co. to the Department of Chemistry, Amherst College.

[1] Abbreviations: Tf, transferrin; Gd–Tf, gadolinium(III)–transferrin; Fe–Tf, iron(III)–transferrin; ESR, electron spin resonance; NMRD, nuclear magnetic relaxation dispersion; kDa, kilodalton(s); Tris-HCl, tris(hydroxymethyl)aminomethane hydrochloride; Hepes, *N*-(2-hydroxyethyl)piperazine-*N*′-2-ethanesulfonic acid; EXAFS, extended X-ray absorption fine structure.

0006-2960/86/0425-1445$01.50/0

is apparently insensitive to the ligand environment in these complexes. An additional anisotropic transition at $g > 2$ has been observed for Gd(III) complexes with pyridine 2,6-dicarboxylate (Geraldes & Williams, 1977). In DNA, a small resonance at $g = 5.9$ was observed in addition to a $g = 2.0$ resonance (Walsh et al., 1963). In the present work, we have found a unique Gd(III) ESR spectrum for Gd–Tf, with no distinct $g = 2.0$ transition but a large $g = 4.96$ transition, which we have used to monitor the pH dependence of the specific binding of Gd(III) to Tf. Since the absence of the $g = 2.0$ signal indicates distortions of the $4f^7$ system of Gd(III) from spherical symmetry, the positions and intensities of the major transitions were calculated by using a strong crystal field Hamiltonian (see eq 1 under Results and Analysis). A good fit, consistent with the observed ESR spectrum, was obtained by using the same crystal field asymmetry parameter previously derived for Fe–Tf (Aasa, 1970).

NMRD, a technique that probes the interaction of solvent molecules with the metal binding site and is thus often a more extensive probe than UV or ESR, was used to characterize another aspect of the Gd(III) environment in transferrin. The technique examines changes in the magnetic relaxation rate of solvent protons as a function of magnetic field, in the presence of solute paramagnetic metals which, in this case, are complexed with protein. The dominant interaction is that of the magnetic dipole of the metal ion with the proton moments of a coordinated water. When this bound water is in relatively rapid exchange with solvent, the relaxation rate of the solvent protons is significantly enhanced. If exchange is slow, little or no relaxation enhancement is observed. A description and review of the relevant experimental and theoretical aspects of Gd(III) complexes have been presented recently (Koenig & Brown, 1984a; Koenig et al., 1984). The relaxation enhancement is dependent on the number of protons found near the metal ions, their distances from the ions, their residence lifetimes on the metal, the orientational relaxation time of the protein, and the magnetic relaxation times of the electronic spin moments. The number of assumptions needed for Gd(III) in Gd–Tf precludes a meaningful quantitative comparison of the data with theory. However, the observed NMRD profile itself can be used to discriminate between Gd(III) in solution, Gd(III) bound to nonspecific sites on the protein, and Gd(III) bound to either of the specific metal-binding sites on the protein. The NMRD signal proved a sensitive monitor of the redistribution of Gd(III) among these environments as the pH was raised from 6.5 [Gd(III) predominantly in solution] to 8.5 [Gd(III) in specific sites in Tf). It is to be stressed that the conclusions from the NMRD data are independent of the ability of relaxation theory to describe the data.

Experimental Procedures

Human serum transferrin was purchased as the apoprotein from both Sigma and Calbiochem-Behring. Gel electrophoresis showed one band for both. Preliminary titration experiments showed that no further purification was necessary for protein from one source (Calbiochem-Behring), whereas protein from another source (Sigma) had to be dialyzed extensively before use to remove adventitious metal chelates. $GdCl_3 \cdot 6H_2O$ (99.999%) was purchased from Aldrich Chemical Co. and vacuum desiccated before use. All other buffers and salts were of the highest research grade available, and all water used was doubly deionized and distilled.

UV Measurements. Optical data were obtained by using a Cary 214 spectrophotometer. Protein samples were approximately 10 μM, and $E^{1\%}_{280\,nm} = 11.2$ was used for the apoprotein (Aisen, 1973). The specific binding of Gd(III) to transferrin was monitored by the ΔOD_{245} in 25 mM Tris-HCl and 10 mM $NaHCO_3$ at pH 8.5 and in 25 mM Hepes and 20 mM $NaHCO_3$ at pH 6.8. Potential problems arising from the interaction of solute Gd(III) with bicarbonate are discussed below.

Nuclear Magnetic Relaxation Dispersion Measurements. The NMRD technique measures the longitudinal relaxation rate, $1/T_1$, of solvent protons as a function of magnetic field, in the present case from 2×10^{-4} to 1.2 T (0.01–50-MHz proton Larmor frequency). Limited descriptions of the apparatus and methods of data collection are given elsewhere [Brown et al., 1977; see Hallenga & Koenig (1976) and references cited therein]. Sample volumes ranged from 0.35 to 0.50 mL and contained either 0.125 or 0.250 mM protein. Gd(III) titrations were performed by adding small volumes of $GdCl_3$ stock (5.8 mM) to an apoprotein solution and adjusting the pH, with the concentration of Gd(III) measured by comparison of the relaxivity in a standard buffer with that of a solution whose concentration was determined by atomic absorption. Samples equilibrated for either 0.25 or 48 h had identical relaxation rates, indicating relatively rapid uptake of ions. The shorter equilibration time was used for the pH and metal titrations. Titrations at pH $\geq$8.5 were done with 25 mM Tris-HCl and 10 mM $NaHCO_3$; titrations at pH $\leq$8.5 were done both in 25 mM Hepes and 10 mM $NaHCO_3$ and in 25 mM Tris-HCl and 10 mM $NaHCO_3$. Fe–Tf was prepared as described elsewhere (O'Hara et al., 1981). Buffer, apoprotein, and Fe–Tf controls were measured under similar conditions. Temperature was regulated by circulating freon maintained at 25 °C, unless otherwise noted. In all pH studies, the pH was measured after all additions.

Electron Spin Resonance. ESR measurements were made by using a Varian E-112 9.5-GHz X-band spectrometer at room temperature and at 77 K. An ESR finger Dewar containing liquid nitrogen was used for the low-temperature spectra. A modulation frequency of 100 kHz and an amplitude of 8 G were used in all the studies. Typical parameters were as follows: receiver gain, 2.5×10^3; microwave power, 10 mW; scan time, 8 min with a time constant of 0.3 s. The magnetic field was varied from 0 to 4000 G (0–0.4 T). Samples were 0.5 mL, 5 mM protein, and were prepared as described previously.

Results and Analysis

UV Titration. There are two peaks in the metal protein vs. apoprotein difference spectra (250 and 290 nm) that are characteristic of the tyrosine deprotonation known to accompany metal binding. Figure 1 shows ΔOD_{245} vs. equivalents of Gd(III) per protein at pH 8.5 and 6.8. The spectroscopic change upon addition of Gd(III) is taken as evidence of binding of the Gd(III) specifically at the two iron-binding sites of transferrin. Figure 1 shows that, at pH 8.5, each transferrin binds two Gd(III) stoichiometrically and that the binding is relatively tight. Using $\Delta\epsilon = 8 \times 10^3\ M^{-1}\ cm^{-1}$ for each tyrosinate (Pecoraro et al., 1981), we calculate an average of 2.2 tyrosinates per site at this pH, consistent with data on other metal transferrins, which indicate 2–3 ionized tyrosines at each of the metal-binding sites (Aisen & Listowsky, 1980). Figure 1 also shows that, at pH 6.8, specific binding of Gd(III) to these same sites on the apoprotein is weak.

Experimental ESR. Figure 2 shows the 77 K ESR powder spectrum of Gd–Tf. The main feature of the pattern is the intense signal at $g = 4.96$, about 360 G wide, set on a broad complex background that spans the range $2 < g < 10$. The Gd(III) ESR spectrum was analyzed as a function of both site

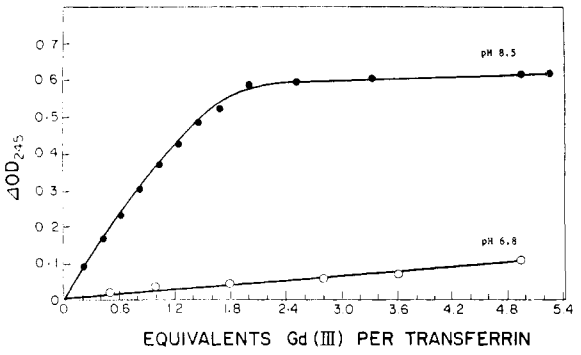

FIGURE 1: ΔOD_{245}, the difference in the absorption of Gd(III)–Tf and apo-Tf at 245 nm, vs. equivalents of Gd(III) per transferrin molecule at pH 8.5 (●) and pH 6.8 (○). Protein concentration was 1.0×10^{-5} M in 25 mM Tris-HCl/10 mM $NaHCO_3$ buffer at pH 8.5 and in 25 mM Hepes/20 mM $NaHCO_3$ buffer at pH 6.8.

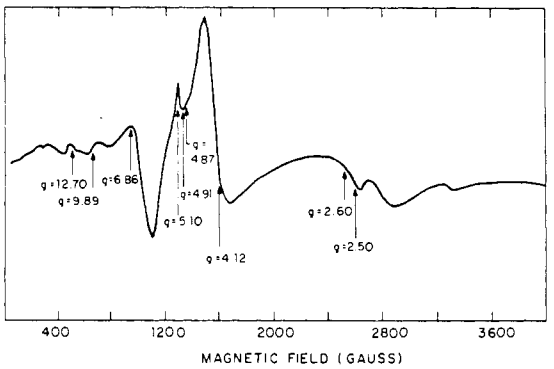

FIGURE 2: Observed 9.5-GHz ESR spectrum of Gd–Tf, pH 8.5, at 77 K. The sample was 5 mM Gd–Tf [1.5 Gd(III)/Tf] in 100 mM Tris/20 mM $NaHCO_3$ buffer, pH 8.5. Arrows show the positions of the calculated g values from Table II.

saturation and pH to determine whether site heterogeneity contributes to the structure in the region of the $g = 4.96$ transition. At pH 8.5, the ESR signal intensity increased linearly with metal addition until 100% saturation, with no change in the shape of the major transition (data not shown). Titration from pH 8.5 to 6.5 resulted in a rapid decrease in signal intensity but, again, with no discernible change in the region of the major transition (data not shown). Although heterogeneity of both binding affinity and ligand symmetry of the sites has been observed for the Fe(III), Cr(III), VO(IV), and Cu(II) environments in Tf by ESR spectroscopy (Chasteen, 1983; Aisen et al., 1969; Cannon & Chasteen, 1975; Zweier & Aisen, 1977), the inequivalence of the sites is not evident in the present ESR results on Gd–Tf.

Theoretical ESR. The spin Hamiltonian was used to describe the Gd(III) ESR spectrum:

$$H = D[S_z^2 - \tfrac{1}{3}S(S+1)] + E(S_x^2 - S_y^2) + g\beta H_0 S \qquad (1)$$

This expression contains terms no greater than second order in the spin components S_x, S_y, and S_z and terms D and E that characterize the most general distortions of the crystal field from octahedral symmetry. The absence of a $g = 2.0$ resonance (Figure 2) indicates that the first two terms are much larger than the Zeeman term. Energies, wave functions, and effective g values were calculated for several different values of $\lambda = E/D$ in the limit $H_0 = 0$ according to the method of Nicklin et al. (1973) assuming that the Zeeman term is negligible. Results consistent with the observed spectrum were obtained for $\lambda = 0.317$, the value found previously for Fe–Tf (Aasa, 1970). Eigenstates and eigenvalues for Gd(III) in Tf for this value for λ are given in Table I. Note that four doubly

Table I: Energy Eigenvalues and Normalized Eigenvectors for the Strong Crystal Field Hamiltonian of Equation 1 for Gd–Tf with $\lambda = 0.317$ and $H_0 = 0$

		eigenvector: $\psi_{i\mu} = a\phi_{\mu 7/2} + b\phi_{\pm 3/2} + c\phi_{\mp 1/2} + d\phi_{\mp 5/2}$				
level	eigenvalue[a]	i	a	b	c	d
1	40.0	1±	−0.933	−0.332	−0.167	−0.105
2	28.0	2±	−0.276	+0.263	+0.525	+0.761
3	10.8	3±	0.251	−0.710	−0.335	+0.567
4	−15.9	4±	0.098	−0.564	−0.765	−0.296

[a] Energy eigenvalue is expressed relative to the energy of the free ion and is in units of the parameter D, measured to be 0.10–0.11 cm^{-1} for Fe–Tf (Pinkowitz & Aisen, 1972).

Table II: Calculated g Values and Relative Transition Intensities for Gadolinium–Transferrin

level	g_{ix}	g_{iy}	g_{iz}	intensity
1	2.60			0.35
				1.69
			12.70	2.04
2	4.91			6.50[a]
		5.10		6.00[a]
			4.87	12.5[a]
3	6.86			1.56
		2.50		11.8
			0.234	[b]
4	9.89			4.24
		4.12		24.4[a]
			1.52×10^{-3}	[b]

[a] These values all contribute to the large $g = 4.96$ resonance and make up 70% of the observable resonances. [b] These transitions are outside the detection range of the X band ESR spectrometer used.

degenerate levels are produced. Table II lists the 12 calculated g values and their relative intensities. The arrows in Figure 2 indicate the positions of these theoretical transitions on the experimental spectrum. The calculation needed to simulate the entire powder pattern of Figure 2 has not been done. The most edifying feature is the clustering of the theoretical values about the observed $g = 4.96$ transition. These clustered values arise both from the nearly isotropic splittings of the E_2 level and from the E_4 level. Combined with the ESR results from Fe(III), Cu(II), Cr(III) and VO(IV), the value of 0.317 for λ indicates a rhombic distortion of the metal-binding sites in Tf from octahedral symmetry that is determined in the main by the protein structure and insensitive to the type of metal ion bound.

NMRD Results. (A) Interaction of Gd(III) with Bicarbonate in Buffer. As shown in Figure 1, binding of Gd(III) to transferrin is strong at pH 8.5 and weak at pH 6.8, even in the presence of bicarbonate. This introduces a potential problem in studying binding of Gd(III) to protein when bicarbonate is present, as seen in Figure 3. The dashed curve represents the NMRD profile of Gd(III)–aquo ions in bicarbonate-free acetate buffer, final pH 6.4. The profile for Gd(III) in bicarbonate-free Hepes buffer, final pH 6.8, is also shown; the slight difference is presumably due to incipient hydrolysis of the water ligands of the aquo ions. [The difference could be due to the difference in buffer, though this is unlikely given the agreement of the dashed curve in Figure 3 with other published data for buffer-free solutions at pH 5.5 [cf. Koenig & Epstein (1975)].] By contrast, addition of 10 mM bicarbonate reduces the relaxivity somewhat at pH 5.5 and eliminates the relaxivity contribution at pH 6.9, ostensibly due to formation and precipitation of $Gd_2(CO_3)_3$. The insolubility of lanthanide carbonates has been reported (Weast, 1972). This point is germane to what follows and, as an aside, is important to the field of NMR imaging, where Gd(III)

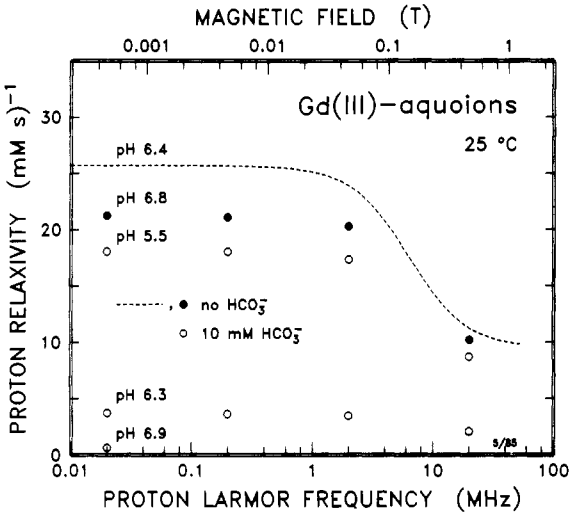

FIGURE 3: Dashed curve is the $1/T_1$ NMRD profile of Gd(III) aquo ions in 0.1 M acetate buffer, pH 6.4 [after Koenig & Brown (1984b)], and the closed circles (●) are the profile in 25 mM Hepes, pH 6.8, both in the absence of HCO_3^-. The remaining data (○) are the profiles at various pHs, all in 25 mM Hepes buffer/10 mM $NaHCO_3$. The data are expressed in relaxivity units, the incremental increase in relaxation rate per millimolar added Gd(III). The approximate concentration of Gd(III) added was 0.34 mM.

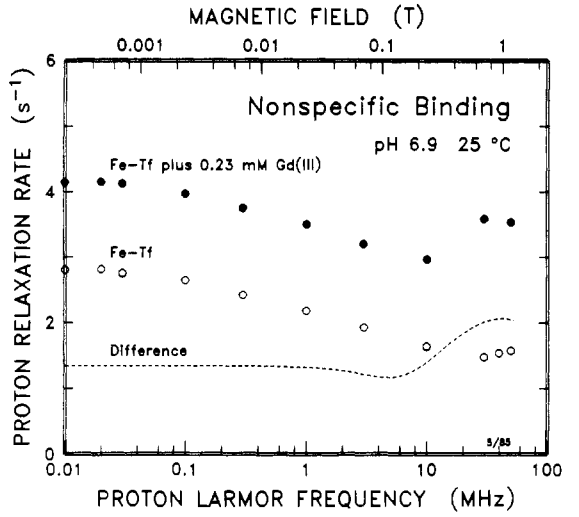

FIGURE 4: NMRD profiles of 0.25 mM Fe–Tf (○) and the same sample with 0.23 mM Gd(III) added (●), at 25 °C, in 25 mM Hepes/10 mM $NaHCO_3$ buffer, pH 6.9. The dahsed line represents the difference between the two measured profiles and demonstrates the presence of nonspecific binding of Gd(III).

complexes are now popular for enhancing image contrast. Gd(III), as both the aquo ion or as the weakly chelated form, would be precipitated by the bicarbonate in blood under physiological conditions.

(B) Nonspecific Binding of Gd(III) to Transferrin. Figure 4 shows that Gd(III) binds to nonspecific sites of Tf at pH 6.9. Gd(III) (0.23 mM), added to Tf saturated with Fe(III) in buffer containing 10 mM bicarbonate, is seen to increase the relaxivity at all values of magnetic field. The difference between the two sets of data, indicated by the dashed curve, is the paramagnetic contribution to the NMRD profile of protein-bound Gd(III) since subtraction eliminates both the contribution of the apoprotein and the considerable background of the specifically bound Fe(III) (Koenig & Schillinger, 1969a,b). The form of the difference profile resembles that of other Gd(III)–protein complexes (Koenig & Brown, 1984b; Lauffer et al., 1985). The mean relaxivity of about 6 mM^{-1} s^{-1} is, however, an order of magnitude lower than that expected,

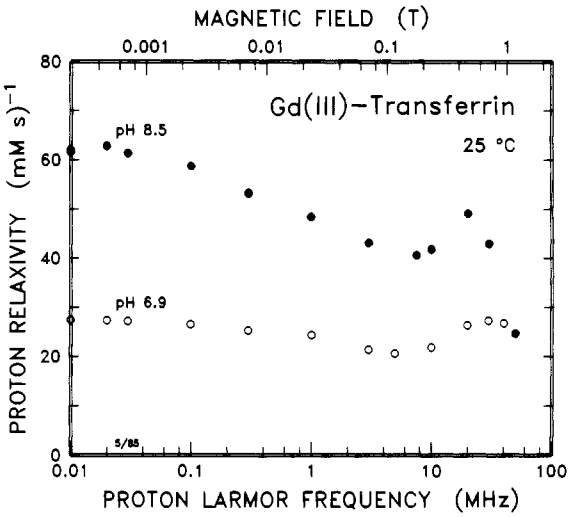

FIGURE 5: NMRD profiles of 0.125 mM apo-Tf plus 0.113 mM Gd(III) at pH 8.5 (●) and of 0.25 mM apo-Tf plus 0.342 mM Gd(III) at pH 6.9 (○), at 25 °C. The buffer was 25 mM Tris/10 mM $NaHCO_3$.

suggesting that approximately 10% of the Gd(III) is complexed with transferrin in nonspecific sites and that the remainder is precipitated as the carbonate.

(C) Comparison of Gd(III) Binding to Transferrin at pH 8.5 and 6.9. Figure 5 shows the paramagnetic contribution to the NMRD profiles of Gd(III) added to apotransferrin at high and low pH. The NMRD profiles of the apoprotein were measured in separate experiments, and the appropriate corrections, though minor, were made. At high pH, the binding is tight, sufficiently so that, as indicated by the results of Figure 1, the specific sites of transferrin compete successfully, both kinetically and thermodynamically, with (bi)carbonate for the Gd(III) ions. Both the large value for the relaxivity (62 mM^{-1} s^{-1} at 0.01 MHz) and the atypical NMRD profile suggest a unique environment for Gd(III) in Tf. The low-pH profile presumably includes contributions from both specifically and nonspecifically bound Gd(III). The much higher relaxivity than estimated from the purely nonspecific sites shown in Figure 4 indicates that some binding of Gd(III) to the specific sites of transferrin must occur even at this low pH. Nonetheless, the mean relaxivity is still somewhat low for Gd(III)–protein complexes, consistent with the optical data (Figure 1) which indicates that binding of Gd(III) at the Fe(III) sites is very weak at pH 6.9.

The symmetry of the ligand field at the specific sites of transferrin is highly rhombic, as evidenced by ESR results mentioned previously and as shown in Figure 2. The theoretical interpretation of NMRD profiles, more specifically, a quantitative comparison of data and theory, becomes very difficult under these circumstances of large ligand field asymmetries (Koenig et al., 1971; Koenig, 1978). Indeed, it is only recently that a quantitative analysis has been made of the profiles of Cu(II)– and VO(II)–Tf (Bertini et al., 1985). A comparable analysis of the pH 8.5 profile for Gd–Tf (Figure 5) will also be very difficult, since the structure of the equations, with the usual simplifying assumptions, cannot account for a high-field relaxivity peak that is lower in magnitude than the low-field value (Gaber et al., 1972; Koenig et al., 1973). Nonetheless, a rough analysis can be made, following Koenig et al. (1973), by noting that at the relaxivity peak near 20 MHz, the condition $\omega_1\tau_c \approx 0.7$ holds, where $\omega_1 = 2\pi(20\text{ MHz})$ and τ_c is a correlation time that enters into the theory. Adding the fact (not shown) that the paramagnetic relaxivities decrease with increasing temperature, which argues that exchange

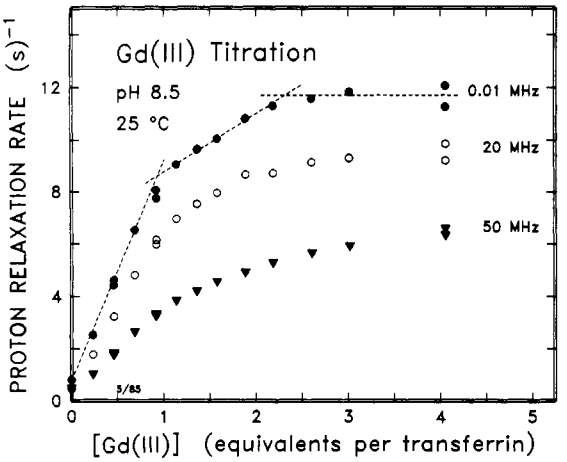

FIGURE 6: Relaxation rates at 0.01 (●), 20 (○), and 50 (▼) MHz of a solution of 0.124 mM apo-Tf, pH 8.5, in 25 mM Tris/10 mM $NaHCO_3$ as a function of added Gd(III), at 25 °C. The dashed lines are meant to emphasize that there are three regimes in the titration data: a steep close up to 1/1 stoichiometry, an intermediate slope from 1/1 to 2/1 stoichiometry, and a relatively flat region beyond.

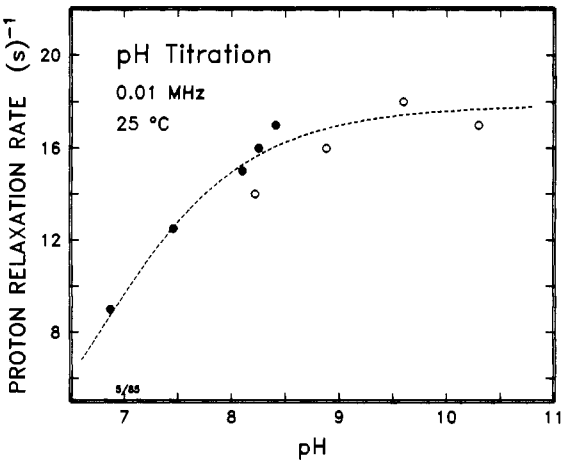

FIGURE 7: Variation of relaxation rate at 0.01 MHz for a sample of 0.25 mM apo-Tf plus 0.35 mM Gd(III) in 25 mM Tris/10 mM $NaHCO_3$ as a function of pH at 25 °C. The initial pH of 8.4 was first reduced in steps to a final pH of 6.87 (●); the back-titration (○) included points from pH 8 to 10.3. The dotted curve through the data is meant to characterize the average behavior of the data but has no theoretical basis.

limitations are not important, one can estimate r, the Gd(III)–proton separation, for a water ligand on the ion; the result is 3.6 Å. This calculation assumes a single such water ligand with its two protons equidistant from the Gd(III). The distance would be 10% less for a single proton as, for example, from a second-sphere water molecule hydrogen bonded with only one proton near the Gd(III), analogous to the outer-sphere mechanism for relaxation that operates in fluoromethemoglobin (Koenig et al., 1981) and presumably Cu(II)–, VO(IV)–, and Fe(III)–Tf (Bertini et al., 1985).

(D) Titration of Gd(III) into Apo-Tf at High pH. Figure 6 shows the relaxation rates at three fields (0.01, 20, and 50 MHz) as Gd(III) is added to a solution of 0.125 mM apo-Tf at pH 8.5. The dashed lines emphasize that the data can be separated into three regimes: a region up to 1/1 stoichiometry, for which the slopes are large, corresponding to the relaxivities observed in Figure 5; a region between 1/1 and 2/1 stoichiometry, with lower (average) relaxivities; and a flat region beyond 2/1 stoichiometry, in which precipitation of Gd(III) is ostensibly occurring.

Judging from the UV titration of Figure 1, 2 equiv of Gd(III) is bound tightly and stoichiometrically to apo-Tf at pH 8.5. Yet the NMRD titration (Figure 6) shows that these bound metal ions are not identical in their contribution to solvent proton relaxation. This can be explained by invoking either sequential binding of Gd(III) to two inequivalent sites on Tf [e.g., Gd(III) binds first to the A site, which has its own characteristic relaxivity, and then to the B site, which has a different characteristic relaxivity] or negative cooperativity [e.g., the first Gd(III) binds to *either* the A or the B site of an apoprotein to produce a characteristic monosubstituted relaxivity, and when all of the proteins have one metal, the monosubstituted Tf binds the second equivalent to produce the disubstituted Tf which has its own characteristic relaxation].

(E) pH Titration of Gd–Tf. Figure 7 shows the effect of sequentially lowering and then raising the pH of a solution of Gd–Tf (initially at pH 8.5) on the bulk proton relaxation rate. Inspection of the resulting pH profile suggests that deprotonation of at least one and maybe several groups on the protein complex is necessary for Gd(III) to be bound in such a way as to generate the characteristic proton relaxivity of Figure 5. These changes are essentially complete at pH 8.5. Possible candidates for this deprotonation are the tyrosine ligands known to chelate the metal and whose complete deprotonation by metal is indicated in Figure 1, a coordinated water molecule whose deprotonation results in a more facile outer-sphere water proton exchange and thus increases the solvent relaxation, or finally, the synergistic bicarbonate anion, whose deprotonation to carbonate in some way facilitates metal binding and solvent relaxation. The displacement of the minimum pH necessary for production of the disubstituted protein from pH 7.0 to 8.5 when substituting Gd(III) for Fe(III) in Tf may reflect the relative Lewis acidities of the two metals.

Discussion

The optical and ESR results taken together indicate that the ligand environments of Gd(III) and Fe(III) in transferrin are very similar, with the same number (two) of tyrosinate ligands, 2/1 ion/protein stoichiometry, and an asymmetric, rhombic crystal field. This argues for the ability of lanthanide-substituted transferrins to serve as models or structural analogues for Fe–Tf at high pH, thereby allowing one to use a wider range of physical measurements to elucidate the nature of metal binding to transferrin. An important difference is that one must go to higher values of pH, approximately pH 8, to get specific, stoichiometric binding of Gd(III) to the two specific Fe(III) sites of transferrin. At lower values of pH, the study of lanthanide binding is complicated by the fact that the mandatory bicarbonate required for specific binding combines with the aquolanthanides to form the insoluble precipitate.

We find that near physiological pH, the interaction of Gd(III) with apo-Tf is complex, involving competition between specific sites, nonspecific sites, and precipitation by bicarbonate. We have no estimate of either the nature or the number of nonspecific sites, though their NMRD profiles are similar to those of other (presumably octahedral) Gd(III)–protein complexes. These sites most likely do not involve ligation by a tyrosine residue, since very little change in the optical spectra was observed at this pH. A nonspecific site for VO(IV) on Tf has previously been reported (Mazurier et al., 1983).

Our NMRD results show that the metal-binding site on transferrin is accessible to rapidly exchanging water protons at a metal to proton distance of 3.3–3.6 Å. A model for the

iron-binding site of transferrin that is consistent with all of our results on Gd–Tf includes two tyrosine ligands whose deprotonation and subsequent tight metal chelation occur near pH 8 and a water molecule ligand whose deprotonation to the hydroxide occurs at a similar pH (~8.5). This model is consistent with that proposed from spectroscopic studies on Fe–Tf by Raymond and co-workers (Pecararo et al., 1981). In addition, the increase in solvent proton relaxivity above pH 8.5 suggests the presence of a water molecule at 3.2 Å which is hydrogen bonded to the coordinated hydroxide. Other evidence for this outer- or second-sphere ligand comes from recent EXAFS work in which a large scatterer at 3.3 Å was observed (Schneider et al., 1984).

Finally, transferrin has shown itself once again to have a very unusual environment for bound metals. Both the ESR spectrum and the NMRD profile for Gd(III) in transferrin are unique, unlike any reported for other biochemical systems and model compounds.

ACKNOWLEDGMENTS

We thank Richard Bersohn for many helpful discussions.

Registry No. Fe, 7439-89-6; HCO_3^-, 71-52-3.

REFERENCES

Aasa, R. (1970) *J. Chem. Phys. 52*, 3919–3930.

Aisen, P. (1973) in *Inorganic Biochemistry* (Eichorn, G., Ed.) p 720, Elsevier, New York.

Aisen, P., & Listowsky, I. (1980) *Annu. Rev. Biochem. 49*, 357–393.

Aisen, P., Aasa, R., & Redfield, A. G. (1969) *J. Biol. Chem. 244*, 4628–4633.

Bertini, I., Briganti, F., Koenig, S. H., & Luchinat, C. (1985) *Biochemistry 24*, 6287–6290.

Brown, R. D., Brewer, C. F., & Koenig, S. H. (1977) *Biochemistry 16*, 3883–3896.

Cannon, J. C., & Chasteen, N. D. (1975) *Biochemistry 14*, 4573–4577.

Chasteen, N. D. (1983) in *Advances in Inorganic Biochemistry* (Theils, E., Eichorn, G., & Margillis, X., Eds.) pp 201–233, Elsevier, New York.

DeLucas, L. J., Suddath, F. L., Grams, R. A., & Bugg, C. E. (1980) *J. Mol. Biol. 123*, 285–286.

Donovan, J. W., & Ross, K. D. (1975) *J. Biol. Chem. 250*, 6022–6025.

Gaber, B. P., Brown, R. D., Koenig, S. H., & Fee, J. A. (1972) *Biochim. Biophys. Acta 271*, 1–5.

Geraldes, E. C., & Williams, R. J. P. (1977) *J. Chem. Soc., Dalton Trans. 18*, 1721–1726.

Hallenga, K., & Koenig, S. H. (1976) *Biochemistry 15*, 4255–4264.

Harris, D. C. (1977) in *Proteins of Iron Metabolism* (Brown, E. B., Ed.) pp 197–217, Grune & Stratton, New York.

Koenig, S. H. (1978) *J. Magn. Reson. 31*, 1–10.

Koenig, S. H., & Schillinger, W. E. (1969a) *J. Biol. Chem. 244*, 3283–3289.

Koenig, S. H., & Schillinger, W. E. (1969b) *J. Biol. Chem. 244*, 6250–6526.

Koenig, S. H., & Epstein, M. (1975) *J. Chem. Phys. 63*, 2279–2284.

Koenig, S. H., & Brown, R. D. (1984a) *Magn. Reson. Med. 1*, 478–495.

Koenig, S. H., & Brown, R. D. (1984b) *Magn. Reson. Med. 1*, 437–449.

Koenig, S. H., Brown, R. D., & Studebaker, J. (1971) *Cold Spring Harbor Symp. Quant. Biol. 36*, 551–555.

Koenig, S. H., Brown, R. D., & Brewer, C. F. (1973) *Proc. Natl. Acad. Sci. U.S.A. 70*, 475–479.

Koenig, S. H., Brown, R. D., & Lindstrom, T. R. (1981) *Biophys. J. 34*, 397–407.

Koenig, S. H., Baglin, C., & Brown, R. D. (1984) *Magn. Reson. Med. 1*, 496–501.

Kojima, N., & Bates, G. W. (1979) *J. Biol. Chem. 25*, 8847–8854.

Lauffer, R. B., Brady, P. J., Brown, R. D., Baglin, C., & Koenig, S. H. (1985) *Magn. Reson. Med.* (submitted for publication).

Luk, C. K. (1971) *Biochemistry 10*, 2838–2843.

MacGillivray, R. T. A., Mendee, E., Shewale, J. G., Sinha, S. K., Lineback-Zins, J., & Brew, K. (1983) *J. Biol. Chem. 258*, 3543–3546.

Mazurier, J., Lhoste, J. M., Montreuil, J., & Spik, G. (1983) *Biochim. Biophys. Acta 745*, 44–49.

Nicklin, R. C., Johnstone, J. K., Barnes, R. G., & Wilder, D. R. (1973) *J. Chem. Phys. 59*, 1652–1668.

O'Hara, P. B., & Bersohn, R. (1982) *Biochemistry 21*, 5296–5299.

O'Hara, P. B., Yeh, S. H., Meares, C. M., & Bersohn, R. (1981) *Biochemistry 20*, 4704–4708.

Pecoraro, V. L., Harris, W. R., Carraro, C. J., & Raymond, K. N. (1981) *Biochemistry 20*, 7033–7039.

Pinkowitz, R. A., & Aisen, P. (1972) *J. Biol. Chem. 247*, 7830–7834.

Reed, G. H., Hershberg, R. D., & DeHaas, G. H. (1979) in *NMR in Biochemistry Symposium*, pp 357–368, Marcel Dekker, New York.

Schneider, D. J., Roe, A. L., Mayer, R. J., & Que, L. (1984) *J. Biol. Chem. 259*, 9699–9703.

Stephens, E. M., & Grisham, C. M. (1979) *Biochemistry 18*, 4876–4885.

Walsh, W., Rupp, L. W., & Wyluda, B. (1963) in *The First International Conference on Paramagnetic Resonance* (Low, Ed.) pp 836–854, Academic Press, New York.

Weast, R. C., Ed. (1972) *Handbook of Chemistry and Physics*, Chemical Rubber Publishing Co., Cleveland, OH.

Zweier, J. L., & Aisen, P. (1977) *J. Biol. Chem. 252*, 6090–6096.